

Phosphorus Chemistry

Nacnac-Cobalt-Mediated P₄ TransformationsFabian Spitzer,^[a] Christian Graßl,^[a] Gábor Balázs,^[a] Eric Mädl,^[a] Martin Keilwerth,^[b]
Eva M. Zolnhofer,^[b] Karsten Meyer,^[b] and Manfred Scheer^{*,[a]}

Dedicated to Professor Walter Frank on the occasion of his 60th birthday

Abstract: A comparison of P₄ activations mediated by low-valent β-diketiminato (L) cobalt complexes is presented. The formal Co⁰ source [K₂(L³Co)₂(μ₂:η¹,η¹-N₂)] (1) reacts with P₄ to form a mixture of the monoanionic complexes [K(thf)₆][L³Co)₂(μ₂:η⁴,η⁴-P₄)] (2) and [K(thf)₆][L³Co)₂(μ₂:η³,η³-P₃)] (3). The analogue Co^I precursor [L³Co(tol)] (4a), however, selectively yields the corresponding neutral derivative [(L³Co)₂(μ₂:η⁴,η⁴-P₄)] (5a). Compound 5a undergoes thermal P atom loss to form the unprecedented complex [(L³Co)₂(μ₂:η³,η³-P₃)] (6). The products 2 and 3 can be ob-

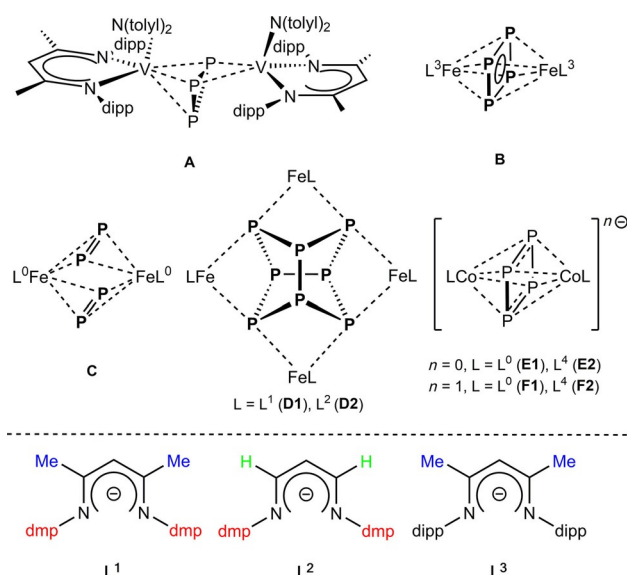
tained selectively by an one-electron reduction of their neutral precursors 5a and 6, respectively. The electrochemical behaviour of 2, 3, 5a, and 6 is monitored by cyclic voltammetry and their magnetism is examined by SQUID measurements and the Evans method. The initial Co^I-mediated P₄ activation is not influenced by applying the structurally different ligands L¹ and L², which is proven by the formation of the isostructural products [(LCo)₂(μ₂:η⁴,η⁴-P₄)] [L = L³ (5a), L¹ (5b), L² (5c)].

Introduction

The activation of white phosphorus (P₄) with transition metal (TM) complexes with the objective of generating organophosphorus compounds has been an ongoing research topic.^[1] For this purpose, an understanding of the P₄ transformation pathway in the coordination sphere of transition metals is necessary. Thus, a variety of P_n ligand moieties were stabilized to give insight into the stepwise P₄ degradation and aggregation processes using well-established ligand systems such as the Cp^R family (Cp = cyclopentadienyl).^[1] However, over the last years, β-diketiminato (nacnac = L) ligand systems have gained increasing attention in mild P₄ activations using M^I precursors: The initial P₄ fixation step of an intact P₄ tetrahedron at a metal center was achieved at an electron-rich Cu^I nacnac compound.^[2] In reactions with transition metal complexes of

Groups 5^[3] and 8–10,^[4] products with modified [P₂]²⁻, [P₄]⁰, [P₄]²⁻ and [P₃]⁴⁻ ligands, respectively, were obtained. So far, for nacnac systems, a [P₃]³⁻ ligand was found solely in compound [(L³VR)₂(cyclo-P₃)]ⁿ⁻ (R = N(tolyl)₂, n = 0, 1; R = O(dipp), n = 0) and [(L³V(N(tolyl)₂)₂)(μ₂:η³,η²-cyclo-P₃)] (A, Scheme 1).^[3c]

However, cyclo-P₃ complexes of the type [LM(μ₂:η³,η³-P₃)M'L']^{±n} have been structurally characterized using neutral, tridentate triphos (1,1,1-tris(diphenylphosphinomethyl)ethane)



Scheme 1. Selected examples of P_n-TM complexes containing ligands L⁰-L⁴ (L⁰ = CH[CHN(2,6-*i*Pr₂C₆H₃)₂], L¹ = CH[C(Me)N(2,6-Me₂C₆H₃)₂], L² = CH[CHN(2,6-Me₂C₆H₃)₂], L³ = CH[C(Me)N(2,6-*i*Pr₂C₆H₃)₂], L⁴ = CH[C(Me)N(2,6-Et₂C₆H₃)₂]). Bottom: Comparison of the nacnac ligands used in this study, L¹, L² and L³.^[5]

[a] F. Spitzer, Dr. C. Graßl, Dr. G. Balázs, Dr. E. Mädl, Prof. Dr. M. Scheer
Institut für Anorganische Chemie, Universität Regensburg
Universitätsstrasse 31, 93040 Regensburg (Germany)
E-mail: manfred.scheer@chemie.uni-regensburg.de
Homepage: <http://www.uni-regensburg.de/chemie-pharmazie/anorganische-chemie-scheer/>

[b] M. Keilwerth, E. M. Zolnhofer, Prof. Dr. K. Meyer
Department of Chemistry and Pharmacy, Inorganic Chemistry
Friedrich-Alexander University Erlangen-Nürnberg (FAU)
Egerlandstrasse 1, 91058 Erlangen (Germany)

Supporting information and the ORCID number(s) for the author(s) of this article can be found under <http://dx.doi.org/10.1002/chem.201605451>.

© 2017 The Authors. Published by Wiley-VCH Verlag GmbH & Co. KGaA. This is an open access article under the terms of Creative Commons Attribution NonCommercial-NoDerivs License, which permits use and distribution in any medium, provided the original work is properly cited, the use is non-commercial and no modifications or adaptations are made.

and etriphos (1,1,1-tris(diethylphosphinomethyl)ethane) ligands in different combinations with 3d metals (Fe, Co, Ni) and 4d metals (Rh, Pd).^[6] The influence of the ligand substituents in Fe^I-mediated P₄ transformation has recently been illustrated by a comparative study using a set of ligands L¹-L³ (Scheme 1).^[7] Despite the application of the same reaction conditions, different products were obtained, which are sensitively dependent on small changes of the ligand substituents. 2,6-Diisopropylphenyl (dipp) substituents as the ligands' aromatic flanking groups support the formation of the dinuclear complexes [(L³Fe)₂(μ₂:η⁴,η⁴-P₄)] (**B**)^[7] and [(L⁰Fe)₂(μ₂:η²,η²-P₂)₂] (**C**).^[4c] The latter was synthesized by the Driess group.^[4c] The ligands L⁰ and L³ only differ in their backbone substituents. However, for sterically less demanding 2,6-dimethylphenyl (dmp) substituents, the formation of the tetranuclear complexes [(LFe)₄(μ₄:η²,η²,η²,η²-P₈)] [L = L¹ (**D1**), L² (**D2**)] with dimerized P₄ units was observed.^[7] These results demonstrate that the product formation is affected by both the aromatic flanking groups and the ligand backbone substituents. Simultaneously, we investigated the [L³Co]-mediated transformations of white phosphorus, which resulted in novel P₄- and P₃-containing complexes (vide infra). In the meantime, Driess and co-workers reported P₄ activation by [LCo] fragments leading to the neutral complexes [(LCo)₂(μ₂:η⁴,η⁴-P₄)] [L = L⁰ (**E1**), L⁴ (**E2**)] (Scheme 1).^[4b] One-electron reduction led to the monoanionic products [K(dme)₄][(LCo)₂(μ₂:η⁴,η⁴-P₄)] [L = L⁰ (**F1**), L⁴ (**F2**)] and transformed the [P₄]⁰ middle deck into a [P₄]²⁻ ligand. Recently, Wolf and co-workers have reported on [(BIAN)Co]⁻-mediated P₄ activations with a nacnac-related bidentate redox non-innocent BIAN (1,2-bis(2,6-diisopropylphenylimino)acenaphthene) ligand system yielding compounds containing [P₄]⁴⁻ moieties.^[8]

Motivated by our first results with [L³Co] compounds, we speculated that the P₄ activation outcome should be sensitive to the oxidation state of the precursor (Co⁰ versus Co^I). Additionally, we wanted to address the question of the ligands' influence (L¹-L³) in Co^I-mediated P₄ activations and we were intrigued by the observed P-atom extrusion from the initially obtained P₄ middle deck to form P₃ compounds. The latter ones are still quite rare in comparison to P₄ ligand complexes.

Here, we report on the P₄ activation by a formal Co⁰ precursor yielding the monoanionic [K(thf)₆][(L³Co)₂(μ₂:η⁴,η⁴-P₄)] (**2**) and [K(thf)₆][(L³Co)₂(μ₂:η³,η³-P₃)] (**3**). Through a Co^I-mediated P₄ transformation at room temperature or under thermolytic conditions, the corresponding neutral relatives are obtained, which generate **2** and **3** selectively after subsequent one-electron reduction. The redox chemistry of the products was investigated by cyclic voltammetry (CV), and their magnetic behavior was examined both in solution (Evans method) and in the solid state (SQUID).

Results and Discussion

The formal Co⁰ precursor [K₂(L³Co)₂(μ₂:η¹,η¹-N₂)] (**1**) was synthesized by a one-pot reaction and was isolated as two different solvomorphs, **1**-solv (solv = *n*-hexane^[9] or OEt₂).^[10] The X-ray structures of **1**-solv consist of two [L³Co] fragments bridged by a N₂ unit. Two potassium atoms cover the N₂ moiety and are

coordinated in the phenyl pockets of the dipp substituents.^[11] The N–N distance in **1**-*n*-hexane/OEt₂ is 1.215(3) and 1.220(4) Å, respectively, which is in line with the that (1.220(2) Å) of the previously reported [K₂(L⁵Co)₂(μ₂:η¹,η¹-N₂)] [L⁵ = CH[C(tBu)N(2,6-*i*Pr₂C₆H₃)₂]₂].^[12] The presence of a [N₂]²⁻ moiety in **1**-*n*-hexane is supported by Raman spectroscopy (ν_{NN} = 1568 cm⁻¹).^[9] The reaction of **1** with P₄ proceeds by N₂ evolution, showing that the formal [N₂]²⁻ species is re-oxidized and revealing **1** as a formal dicobalt(0) starting material.

Conducting the reaction in 1:1 stoichiometry leads to the complete consumption of P₄ and the formation of a mixture of the monoanionic complexes [K(thf)₆][(L³Co)₂(μ₂:η⁴,η⁴-P₄)] (**2**) and [K(thf)₆][(L³Co)₂(μ₂:η³,η³-P₃)] (**3**), which were detected by ¹H NMR spectroscopy.^[13] The appearance of a *cyclo*-P₃ moiety in product **3** indicates that an extrusion of one P atom from the *cyclo*-P₄ moiety in **2** is possible. However, if the reaction is conducted with two equivalents of P₄, compound **2** is the only product found in the ¹H NMR spectrum.

The solid state structure of **2**:2 thf reveals a salt consisting of two [K(thf)₆]⁺ cations and two crystallographically distinguishable [(L³Co)₂(μ₂:η⁴,η⁴-P₄)]⁻ monoanions (Figure 1).^[9] Each anion is a centrosymmetric dicobalt complex that consists of two [L³Co] fragments bridged by a planar *cyclo*-P₄ ligand. The P–P

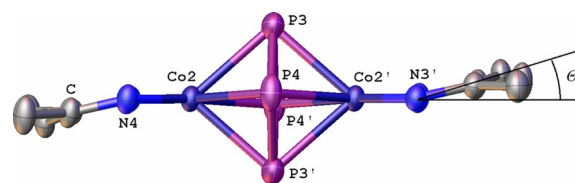


Figure 1. Anionic part of the molecular structure of **2**. Hydrogen atoms and aromatic flanking groups are omitted for clarity; thermal ellipsoids are drawn at 50% probability level. The torsion angle θ is depicted spanning between the Co...Co' axis and the plane formed by the nitrogen atoms and the methine carbon in the ligand backbone.

distances amount to 2.1913(10)–2.1951(10) Å in anion 1 and 2.1897(10)–2.2004(10) Å in anion 2, respectively. These values correspond well with the *cyclo*-[P₄]²⁻ moiety (2.178(1) and 2.207(1) Å) of the reported compound [(L³Fe)₂(μ₂:η⁴,η⁴-P₄)] (**B**).^[7] The central P₄ ligands in **2** are almost square planar with interior angles of 86.07(3) and 93.92(3)^o in anion 1 and 86.38(3) and 93.62(3)^o in anion 2. The Co–P distances range from 2.3362(7)–2.4149(7) Å in anion 1 and 2.3441(7)–2.4190(7) Å in anion 2. Selected atomic distances of compound **2** are summarized in Table 1. Minor deviations within the atomic parameters of compound **2**:2 thf and the related compounds [K(dme)₄][(LCo)₂(μ₂:η⁴,η⁴-P₄)] [L = L⁰ (**F1**), L⁴ (**F2**)] can be explained by small changes in the organic environment of the counter ion and the nacnac ligands of the complex monoanions. They may affect the Co...Co' distances and their coordination geometry (torsion angle θ between the Co...Co' axis and the plane formed by the nitrogen atoms and the methine carbon in the ligand backbone; Figure 1 for graphical presentation of θ).^[14]

The monoanionic [(L³Co)₂(μ₂:η³,η³-P₃)]⁻ was obtained in two different solvomorphs [K(dme)₄][(L³Co)₂(μ₂:η³,η³-P₃)]-dme (**3a**)

Table 1. Comparison of P–P and Co...Co' atomic distances and torsion angles θ in anions of $[(\text{L}^0\text{Co})_2(\mu_2\text{-}\eta^4, \eta^4\text{-P}_4)]^-$ ($\text{L} = \text{L}^3$ (**2**)^[9], L^0 (**F1**)^[4b], L^4 (**F2**)^[4b]).

Complex	2:anion 1	2:anion 2	F1 ^[4b]	F2 ^[4b,a]
$d(\text{P}-\text{P})$ [Å]	2.1913(10)	2.1897(10)	2.1739(7)	2.154(1) ^[a]
	2.1951(10)	2.2004(10)	2.1976(7)	2.163(1) ^[a] 2.225(1) ^[a] 2.230(1) ^[a]
$d(\text{Co}\cdots\text{Co}')$ [Å]	3.603	3.625	3.626	3.603
θ [°]	13.87(6)	15.87(6)	15.33(4)	6.60(8) ^[a] 14.97(7) ^[a]

[a] Anion of **F2** is not centrosymmetric. Therefore, four individual $d(\text{P}-\text{P})$ and two θ values are given.

and $[\text{K}(\text{thf})_6][(\text{L}^3\text{Co})_2(\mu_2\text{-}\eta^3, \eta^3\text{-P}_3)]\cdot 2\text{thf}$ (**3b**). Both compounds are ionic and consist of solvent (DME or THF) molecules, one solvent-saturated potassium counter ion, and the $[(\text{L}^3\text{Co})_2(\mu_2\text{-}\eta^3, \eta^3\text{-P}_3)]^-$ monoanion (Figures 2 and 3). In both X-ray structures, the complex anions are built from two $[\text{L}^3\text{Co}]$ fragments bridged

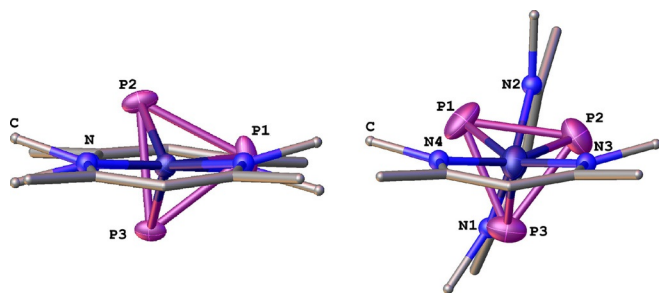


Figure 2. Comparison of the anions in the molecular structures of **3a** (left) and **3b** (right). Hydrogen atoms and aromatic flanking groups are omitted for clarity; thermal ellipsoids of Co and P atoms are drawn at 50% probability level; major component of disordered *cyclo*-P₃ ligand is drawn in **3a**.

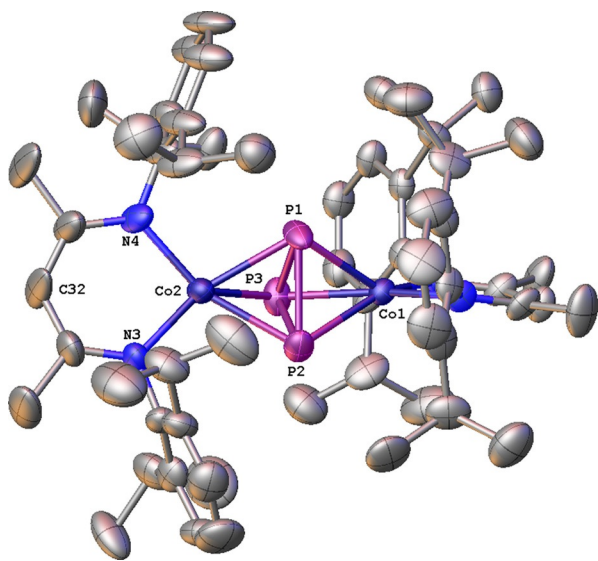


Figure 3. Anionic part of the molecular structure of **3b**. Hydrogen atoms are omitted for clarity; thermal ellipsoids are drawn at 50% probability level.

by a P₃ triangle. In **3a**, the L³ ligand planes are almost parallel to each other with a dihedral angle of 2.00(7)° (N1-N2 versus N3-N4). However, in **3b**, the ligand planes are in a twisted conformation with a dihedral angle of 74.2(4)° (N1-N2 versus N3-N4, Figure 2).

The different complex anion conformations may originate from packing effects directed by the unequally shaped counter cations. The *cyclo*-P₃ middle deck is disordered over two positions in **3a** (occupancy 81:19).^[15] The middle deck in **3b**, however, is localized at one distinct position. As can be seen in Table 2, the P–P distances in **3a** are similar to the ones in the

Table 2. Comparison of selected atomic distances and angles in the $[(\text{L}^3\text{Co})_2(\mu_2\text{-}\eta^3, \eta^3\text{-P}_3)]^-$ anion in **3a** (major component) and **3b**, $[(\text{L}^3\text{V}(\text{N}(\text{tolyl})_2)_2(\mu_2\text{-}\eta^3, \eta^2\text{-cyclo-P}_3))]^-$ (**A**)^[3c] and the dication in $[(\text{triphos})\text{Co}(\mu_2\text{-}\eta^3, \eta^3\text{-cyclo-P}_3)\text{Fe}(\text{etripfos})](\text{PF}_6)_2$ (**G**).^[6b]

Complex	3a	3b	A ^[3c]	G ^[6b]
$d(\text{P}-\text{P})$ [Å]	2.1674(13)	2.217(4)	2.1658(10)	2.226(8)
	2.1790(16)	2.224(4)	2.1804(9)	2.229(8)
	2.3303(17)	2.237(4)	2.2155(9)	2.234(8)
$\angle(\text{P}-\text{P}-\text{P})$ [°]	57.34(5)	59.59(13)	59.03(3)	–
	57.82(5)	59.93(14)	59.68(3)	–
	64.84(5)	60.48(13)	61.29(3)	–
	64.84(5)	60.48(13)	61.29(3)	–
$d(\text{M}\cdots\text{M}')$ [Å]	3.7359(5)	3.724(2)	4.460	3.80
	9.43(7)	8.7(3)	–	–
θ [°]	12.22(7)	13.5(6)	–	–

nacnac containing compound $[(\text{L}^3\text{V}(\text{N}(\text{tolyl})_2)_2(\mu_2\text{-}\eta^3, \eta^2\text{-cyclo-P}_3))]^-$ (**A**),^[3c] displaying a *cyclo*-[P₃]³⁻ moiety. In **3b**, they compare better with the ones in $[(\text{triphos})\text{Co}(\mu_2\text{-}\eta^3, \eta^3\text{-cyclo-P}_3)\text{Fe}(\text{etripfos})](\text{PF}_6)_2$ (**G**).^[6b] Overall, they are in line with P–P single bonds [for comparison: P–P single bond in white phosphorus determined by X-ray diffraction: 2.209(5) Å,^[16] electron diffraction: 2.1994(3) Å,^[17] Raman spectroscopy: 2.2228(5) Å,^[18] and DFT calculations: 2.1994(3) Å^[17]]. The Co–P distances in **3a** are between 2.2046(17) and 2.3684(8) Å and for **3b** in the range of 2.248(3) and 2.277(3) Å. The Co...Co' distance in **3a** is 3.7359(5) and amounts to 3.724(2) Å in **3b**, which is slightly elongated compared to **2** (3.603 and 3.625 Å, Table 1).

The ¹H NMR spectra in [D₈]THF display signals between 11.42 and –35.29 ppm for **2**^[9] and 8.15 and –12.85 ppm for **3**, respectively. Except for the THF and DME signals, respectively, the ¹H NMR spectra of **3a, b** do not deviate from each other. No signals are detected in the ³¹P{¹H} NMR spectra for **2** and **3** due to their paramagnetic nature. Their magnetic moment (μ_{eff}) in [D₈]THF solution (RT) was determined by the Evans method: 3.90 μ_{B} (**2**) and 3.51 μ_{B} (**3**). In the solid state, these values are confirmed by SQUID measurements displaying a gradual decrease of the magnetic moment in the temperature range from 300 to 2 K of 3.80 to 3.30 μ_{B} in **2** and 3.58 to 1.70 μ_{B} in **3a**. Therefore, the electronic structure of **2** is best described as containing a [P₄]²⁻ moiety bridging mixed valence Co^I and Co^{II} centers. This is in agreement with the previously reported compounds **F1** and **F2**.^[4b] Compound **3**, however, contains a [P₃]³⁻ ligand, which is bridged by two Co^{II} metal centers.

As mentioned above, starting from the formal Co^0 precursor **1**, we obtained the compounds **2** and **3** as a mixture of products, the ratio of which is sensitively dependent on stoichiometry and reaction conditions. To discover an alternative approach, we targeted the use of the Co^I starting material $[\text{L}^3\text{Co}(\text{tol})]$ (**4a**), which was speculated to yield the neutral analogues of **2** and **3**. After their one-electron reduction, the compounds **2** and **3** should be accessible.

Therefore, the Co^I compound $[\text{L}^3\text{Co}(\text{tol})]$ (**4a**) was reacted with P_4 and $[(\text{L}^3\text{Co})_2(\mu_2\text{-}\eta^4, \eta^4\text{-P}_4)]$ (**5a**) was selectively formed. Metric parameters and the characterization of compound **5a** are discussed in detail below.

Refluxing **5a** for three hours (110°C , toluene) gives rise to the loss of one phosphorus atom and the formation of $[(\text{L}^3\text{Co})_2(\mu_2\text{-}\eta^3, \eta^3\text{-P}_3)]$ (**6**),^[19] which was clearly characterized by mass spectrometry^[20] and ^1H NMR spectroscopy.^[21] The dinuclear compound contains two $[\text{L}^3\text{Co}]$ fragments, and the bridging middle deck exhibits a savage disorder within its *cyclo*- P_3 moiety. We emphasize that the P–P distances cannot be precisely described. However, the initially localized electron density unambiguously displays triangle-shaped *cyclo*- P_3 constitution and enables an estimation of the P–P distances in **6** (approx. $d(\text{P}–\text{P})$: 2.147(3), 2.223(2), 2.235(2) Å). These values are comparable with the ones found in **3a** (2.1674(13), 2.1790(16), 2.3303(17) Å) and **3b** (2.217(4), 2.224(4) and 2.237(4) Å) and are elongated compared to the ones in **A** (2.1658(10), 2.1804(9) and 2.2155(9) Å).^[3c] The $\text{Co}\cdots\text{Co}'$ distance in **6** is 3.747 Å and therefore comparable to the ones in **3a** (3.7359(5) Å) and **3b** (3.724(2) Å), but elongated compared to its precursor complex **5a** (3.610 Å, *vide infra*).

The ^1H NMR spectrum of **6** reveals signals between 20.06 and -12.68 ppm. No signal is detected in the $^{31}\text{P}\{^1\text{H}\}$ NMR spectrum. The magnetic moment (μ_{eff}) of **6** in C_6D_6 solution is $2.97 \mu_{\text{B}}$ at room temperature (Evans method).^[22] This value is confirmed in the solid state by a SQUID measurement. A successive decrease from 2.7 to $2.0 \mu_{\text{B}}$ was measured in the temperature range from 300 to 2 K (see the Supporting Information). The values are in agreement with antiferromagnetically coupled Co^{II} and Co^{III} metal centers.

Electrochemistry

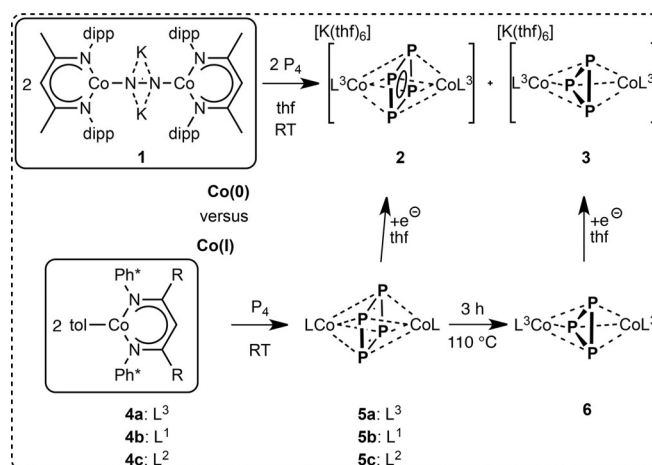
The electrochemical properties of the complexes **5a** and **6** were probed by cyclic voltammetry (CV) in THF solution containing Bu_4NPF_6 electrolyte (0.1 mol L^{-1} , 295 K, see Supporting Information for further details).^[20] An irreversible oxidation was detected at $E_{1/2} = -0.34 \text{ V}$ for **5a** and $E_{1/2} = -0.11 \text{ V}$ for **6** (vs. $\text{Cp}_2\text{Fe}/\text{Cp}_2\text{Fe}^+$). The compounds **5a** and **6** each reveal one reversible reduction at $E_{1/2} = -1.62 \text{ V}$ (vs. $\text{Cp}_2\text{Fe}/\text{Cp}_2\text{Fe}^+$). The complexes **2**^[9] and **3** confirm these values by the corresponding electrochemical behavior. For **3**, an additional reduction event was monitored at -2.52 V (vs. $\text{Cp}_2\text{Fe}/\text{Cp}_2\text{Fe}^+$).

We experimentally performed the reduction of **5a** and **6**, respectively, with one equivalent of potassium graphite in THF at room temperature. The corresponding anionic compounds $[\text{K}(\text{thf})_6][(\text{L}^3\text{Co})_2(\mu_2\text{-}\eta^4, \eta^4\text{-P}_4)]$ (**2**) and $[\text{K}(\text{thf})_6][(\text{L}^3\text{Co})_2(\mu_2\text{-}\eta^3, \eta^3\text{-P}_3)]$ (**3**), respectively, are selectively and quantitatively formed,

which was proven by ^1H NMR spectroscopy of the crude reaction solution. On a preparative scale, the isolated yields obtained as single crystals are 41 % for **2** and 62 % for **3**. Consequently, regarding selectivity, this synthetic route is superior to the Co^0 -mediated P_4 activation, which, in contrast, yielded a mixture of products.

Impact of ligand design

Three β -diketimines (L^1H , L^2H , L^3H) were synthesized to provide a comparable hybrid ligand set $\text{L}^1\text{--L}^3$ with backbone ($\text{R} = \text{H}$, Me) and aromatic ($\text{Ph}^* = \text{dmp}$ or *dipp*) substituents (Scheme 1 and Scheme 2), and to investigate the influence of the ligand



Scheme 2. Performed Co^0 - and Co^I -mediated P_4 transformations.

design on the Co^I -mediated P_4 transformation. The $[\text{LCo}(\text{tol})]$ [$\text{L} = \text{L}^3$ (**4a**), L^1 (**4b**), L^2 (**4c**)] starting materials were prepared in one-pot reactions (see the Supporting Information). All conducted P_4 activation reactions were performed under the same conditions ($[\text{LCo}(\text{tol})]:\text{P}_4 = 2:1$, toluene, 2–3 h, RT) and yielded similar isolated products $[(\text{LCo})_2(\mu_2\text{-}\eta^4, \eta^4\text{-P}_4)]$ [$\text{L} = \text{L}^3$ (**5a**), L^1 (**5b**), L^2 (**5c**)]. The crystals of all the new compounds **5a–c** were grown from saturated toluene solutions, and single crystal X-ray diffraction was performed. The molecular structures of **5a–c** are shown in Figure S5 in the Supporting Information. As a representative, compound **5a** is presented in Figure 4a. Its P_4 moiety is rectangularly shaped, consequently spanned by two shorter and two longer P–P atom distances. Together with two coordinating Co atoms, the $[\text{P}_4\text{Co}_2]$ complex core builds a distorted octahedron. In **5a–c**, the shorter P–P atom distances are between 2.1256(6) and 2.1301(7) Å and the longer P–P distances are between 2.2513(10) and 2.2980(7) Å. Compared with a phosphorus single bond in the tetrahedral P_4 , the planar rectangular-shaped P_4 moieties in **5a–c** contain a pair of shorter and a pair of elongated P–P bonds. The $\text{Co}\cdots\text{Co}'$ distances in **5a–c** are between 3.502 and 3.610 Å and, therefore, any bonding interaction can be ruled out. Due to the centrosymmetric molecular structure ($P2_1/n$ in **5a–c**), the ligands are parallel to each other. In **5a–c**, the torsion angles θ

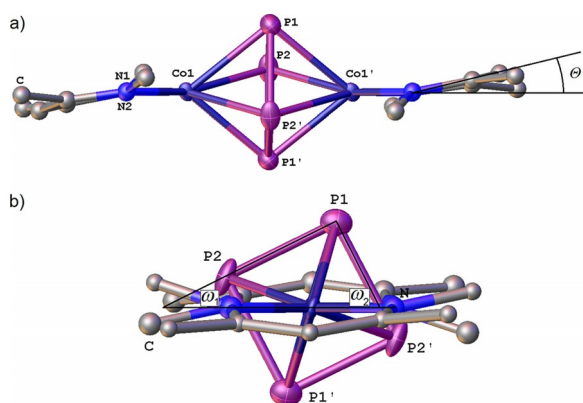


Figure 4. a) Molecular structure of the compound **5a**. Hydrogen atoms and aromatic flanking groups are omitted for clarity; thermal ellipsoids are drawn at 50% probability level. The torsion angle θ is depicted, which spans between the Co...Co' axis and the plane formed by the nitrogen atoms and the methine carbon in the ligand backbone; b) view along Co1...Co1' axis, revealing the angles ω_1 and ω_2 , which span between the N-N axis of coordinating nitrogen atoms and the edges of the *cyclo*-P₄ unit.

(between the Co...Co' axis and the plane formed by the nitrogen atoms and the methine carbon in the ligand backbone) are between 3.40(6) and 12.32(6)°. In **5b,c** (and **E1,2**^[4b]), the P–P edges of the *cyclo*-P₄ unit are nearly parallel or rectangular, respectively, compared to the N–N axis of coordinating nitrogen atoms (compare $\sphericalangle(\text{NN-PP}_{\text{short}}) = \omega_1$ and $\sphericalangle(\text{NN-PP}_{\text{long}}) = \omega_2$, see Figure 4b). The structural parameters of **5a–c** and **E1,2** are summarized in Table 3.

Complex	5a	5b	5c	E1 ^[4b]	E2 ^[4b]
<i>d</i> (P–P) short [Å]	2.1295(10)	2.1256(6)	2.1301(7)	2.1237(13)	2.1298(14)
<i>d</i> (P–P) long [Å]	2.2513(10)	2.2972(6)	2.2980(7)	2.2984(13)	2.2889(15)
<i>d</i> (Co...Co') [Å]	3.610	3.502	3.503	3.491	3.533
θ [°]	12.22(8)	12.32(6)	3.40(6)	14.88(9)	7.0(1)
ω_1 [°]	26.34(6)	2.18(4)	1.97(4)	1.96(7)	2.58(8)
ω_2 [°]	62.36(6)	87.87(4)	87.95(4)	88.02(7)	87.43(8)

The ¹H NMR spectra of the compounds **5a–c** display signals between 11.99 and –28.61 ppm and reveal their paramagnetic nature in solution. Therefore, no signals are detected in their ³¹P{¹H} NMR spectra. Their magnetic moment (μ_{eff}) in solution (RT) was determined by the Evans method: 3.02 μ_{B} (**5a**^[22] in C₆D₆), 2.42 μ_{B} (**5b** in C₆D₆), 1.84 μ_{B} (**5c** in [D₈]THF). In the solid state, however, the SQUID measurements of **5a** and **5b** display diamagnetic behavior in the temperature range of 2–300 K. Their electronic structure in the solid state is best described as two antiferromagnetically coupled Co^I centers bridged by a [P₄]⁰ ligand similar to the previously reported compounds **E1,2**.^[4b] In solution, exclusively one signal set for the ligand is observed in the ¹H NMR spectrum of **5a–c**, respectively, sug-

gesting the integrity of each dinuclear compound in solution on the NMR time scale (Figure S15).

Conclusion

We reported different [LCo^I]-mediated P₄ activations yielding neutral complexes [(LCo)₂(μ₂-η⁴,η⁴-P₄)] (L = L¹, L², L³), each containing a similar rectangular-shaped [P₄]⁰ moiety. In contrast to the P₄ activation by LFe^I compounds, for the Co system, the ligand substituents (L¹–L³) do not alter the reaction outcome. For the ligand system L³, we demonstrate that one P atom can be extruded thermolytically to generate an unprecedented neutral *cyclo*-[P₃]^{3–}-containing compound [(L³Co)₂(μ₂-η³,η³-P₃)]. As a novel approach, we present the P₄ transformation with a formal [L³Co⁰] precursor, which generates corresponding monoanions with *cyclo*-[P₄]^{2–} and *cyclo*-[P₃]^{3–} ligands as a mixture of products. Each product was selectively accessed through the one-electron reduction of its neutral precursor.

Acknowledgements

This work was initially supported by the Deutsche Forschungsgemeinschaft. The European Research Council (ERC) is acknowledged for the support in the SELFPHOS AdG-339072 project. We are thankful to Dr. M. Bodensteiner for his valuable support regarding the solution of X-ray structures. We extend our thanks to Dr. F. Dielmann for the initial X-ray measurement of **5a** and to Dr. W. Patterson for the Raman measurement of 1-*n*-hexane.

Keywords: cyclic voltammetry • paramagnetic NMR • small molecule activation • white phosphorus • β-diketiminates

- [1] a) D. Tofan, B. M. Cossairt, C. C. Cummins, *Inorg. Chem.* **2011**, *50*, 12349–12358; b) M. Caporali, L. Gonsalvi, A. Rossin, M. Peruzzini, *Chem. Rev.* **2010**, *110*, 4178–4235; c) M. Scheer, G. Balázs, A. Seitz, *Chem. Rev.* **2010**, *110*, 4236–4256; d) S. Khan, S. S. Sen, H. W. Roesky, *Chem. Commun.* **2012**, *48*, 2169–2179; e) N. A. Giffin, J. D. Masuda, *Coord. Chem. Rev.* **2011**, *255*, 1342–1359.
- [2] F. Spitzer, M. Sierka, M. Latronico, P. Mastroianni, A. V. Virovets, M. Scheer, *Angew. Chem. Int. Ed.* **2015**, *54*, 4392–4396; *Angew. Chem.* **2015**, *127*, 4467–4472.
- [3] a) B. L. Tran, M. Singhal, H. Park, O. P. Lam, M. Pink, J. Krzystek, A. Ozarowski, J. Telsler, K. Meyer, D. J. Mindiola, *Angew. Chem. Int. Ed.* **2010**, *49*, 9871–9875; *Angew. Chem.* **2010**, *122*, 10067–10071; b) C. Camp, L. Maron, R. G. Bergman, J. Arnold, *J. Am. Chem. Soc.* **2014**, *136*, 17652–17661; c) B. Pinter, K. T. Smith, M. Kamitani, E. M. Zolnhofer, B. L. Tran, S. Fortier, M. Pink, G. Wu, B. C. Manor, K. Meyer, M.-H. Baik, D. J. Mindiola, *J. Am. Chem. Soc.* **2015**, *137*, 15247–15261.
- [4] a) S. Yao, Y. Xiong, C. Milsmann, E. Bill, S. Pfirrmann, C. Limberg, M. Driess, *Chem. Eur. J.* **2010**, *16*, 436–439; b) S. Yao, N. Lindenmaier, Y. Xiong, S. Inoue, T. Szilvási, M. Adelhardt, J. Sutter, K. Meyer, M. Driess, *Angew. Chem.* **2015**, *127*, 1266–1270; c) S. Yao, T. Szilvási, N. Lindenmaier, Y. Xiong, S. Inoue, M. Adelhardt, J. Sutter, K. Meyer, M. Driess, *Chem. Commun.* **2015**, *51*, 6153–6156.
- [5] The ligands L⁰–L⁴ are called “nacnac” in this report due to their structural similarities. More precisely, L⁰ and L² can be regarded as vinylogous amidines and therefore are part of the “vinamidine” ligand family. See: D. Lloyd, H. McNab, *Angew. Chem. Int. Ed. Engl.* **1976**, *15*, 459–468; *Angew. Chem.* **1976**, *88*, 496–504.
- [6] a) For (triphos)Co,Ni(triphos) and (triphos)Ni,Ni(triphos), see: M. Di Vaira, S. Midollini, L. Sacconi, *J. Am. Chem. Soc.* **1979**, *101*, 1757–1763; b) for

- (triphos)Fe,Co(triphos) and (triphos)Co,Co(triphos) (in footnote): C. Bianchini, M. Di Vaira, A. Meli, L. Sacconi, *Inorg. Chem.* **1981**, *20*, 1169–1173; c) for (triphos)Co,Rh(triphos) and (triphos)Ni,Rh(triphos): C. Bianchini, M. Di Vaira, A. Meli, L. Sacconi, *J. Am. Chem. Soc.* **1981**, *103*, 1448–1452; d) for (triphos)Pd,Pd(triphos): P. Dapporto, L. Sacconi, P. Stoppioni, F. Zanobini, *Inorg. Chem.* **1981**, *20*, 3834–3839; e) for a review, see: M. Di Vaira, L. Sacconi, *Angew. Chem. Int. Ed. Engl.* **1982**, *21*, 330–342; *Angew. Chem.* **1982**, *94*, 338–351; for additional examples: f) O. J. Scherer, B. Werner, G. Heckmann, G. Wolmershäuser, *Angew. Chem. Int. Ed. Engl.* **1991**, *30*, 553–555; *Angew. Chem.* **1991**, *103*, 562–563; g) E. Mädl, G. Balázs, E. V. Peresykina, M. Scheer, *Angew. Chem. Int. Ed.* **2016**, *55*, 7702–7707; *Angew. Chem.* **2016**, *128*, 7833–7838; h) Y. Nakanishi, Y. Ishida, H. Kawaguchi, *Inorg. Chem.* **2016**, *55*, 3967–3973.
- [7] F. Spitzer, C. Graßl, G. Balázs, E. M. Zolnhofer, K. Meyer, M. Scheer, *Angew. Chem. Int. Ed.* **2016**, *55*, 4340–4344; *Angew. Chem.* **2016**, *128*, 4412–4416.
- [8] S. Pelties, T. Maier, D. Herrmann, B. de Bruin, C. Rebreyend, S. Gärtner, I. G. Shenderovich, R. Wolf, *Chem. Eur. J.* DOI: 10.1002/chem.201603296.
- [9] F. Spitzer, Master thesis, *University of Regensburg* **2013**.
- [10] After lithiation of L³H and subsequent transmetalation with CoBr₂, its reduction was performed with an excess of potassium graphite under N₂ atmosphere.
- [11] In 1-*n*-hexane the NCCCN ligand planes are orientated parallel to each other. However, in 1-OEt₂, they are twisted (dihedral angle of coordinating N atoms: 32.38(9)°). Further analytical data (X-ray, ¹H NMR, Evans method, EA, Raman spectrum) and pictures of 1-solv are presented in the Supporting Information.
- [12] K. Ding, A. W. Pierpont, W. W. Brennessel, G. Lukat-Rodgers, K. R. Rodgers, T. R. Cundari, E. Bill, P. L. Holland, *J. Am. Chem. Soc.* **2009**, *131*, 9471–9472.
- [13] For initial investigations see reference [9]. The identification of products **2** and **3** in the ¹H NMR spectra was enabled after their selective preparation.
- [14] The dependency of torsion angle θ and Fe...Fe' distance was already recognized in citation [7].
- [15] Due to the disorder of the *cyclo*-P₃ moiety, only the geometric parameters of the major component are discussed. Furthermore, it has to be noted that the positions of the disordered P3 and P3A atoms are close to each other and hence, the involved bond lengths might not be determined with high accuracy.
- [16] In β -P₄: A. Simon, H. Borrmann, H. Craubner, *Phosphorous and Sulfur* **1987**, *30*, 507–510.
- [17] B. M. Cossairt, C. C. Cummins, A. R. Head, D. L. Lichtenberger, R. J. F. Berger, S. A. Hayes, N. W. Mitzel, G. Wu, *J. Am. Chem. Soc.* **2010**, *132*, 8459–8465.
- [18] N. J. Brassington, H. G. M. Edwards, D. A. Long, *J. Raman Spectrosc.* **1981**, *11*, 346–348.
- [19] The crystal structures of **6** and **5a** were initially reported in reference [20]. However, to present improved structural values, crystals of **6** and **5a** were re-measured.
- [20] C. Grassl, PhD thesis, *University of Regensburg*, **2013**.
- [21] During the thermolysis, a black, pyrophoric precipitate is formed. The CHN analysis of the washed and dried precipitate suggests only some organic content (C%: \approx 35, H%: \approx 5, N%: \approx 3). Exclusively, compound **6** and L³H were detected in the ¹H NMR spectrum (reaction control) as the only soluble products formed during the thermolysis reaction.
- [22] For initial investigations see reference [20]. For further information see the Supporting Information.

Manuscript received: November 22, 2016

Accepted Article published: December 29, 2016

Final Article published: January 25, 2017